The Influence of Pulse Rise and Fall Times on *N*-norm Portraits along Power Supply Bus

Ruslan R. Gazizov
Department of Television and Control (TU)
Tomsk State University of Control Systems and Radioelectronics (TUSUR)
Tomsk, Russian Federation
ruslangazizow@gmail.com

Timur T. Gazizov
Department of Television and Control (TU)
Tomsk State University of Control Systems and Radioelectronics (TUSUR)
Tomsk, Russian Federation
timurtsk@gmail.com

Talgat R.Gazizov
Department of Television and Control (TU)
Tomsk State University of Control Systems and Radioelectronics (TUSUR)
Tomsk, Russian Federation
talgat@tu.tusur.ru

***Abstract*—The paper investigates the influence of pulse rise and fall times on *N*-norm portraits calculated along conductors of a spacecraft power supply bus. The values were calculated and portraits of 5 *N*-norms were drawn along a conductor of the power supply bus. It is shown that the change of pulse rise and fall times strongly influences the N_2 norm (up to 100 times) and N_4 norm (up to 4 times) portraits. The other norm portraits are not influenced by the change of pulse rise and fall times.**

***Index Terms*—simulation, ultrashort pulse, *N*-norms, spacecraft power supply bus.**

I. Introduction

Nowadays radioelectronic equipment (REE) is developing at a fast pace, the mounting density of its internal structures [1] and the frequencies of useful and interfering signals are increasing. All of these lead to stricter requirements for electromagnetic compatibility (EMC), since with increasing complexity of REE, the probability of electromagnetic interference that adversely affects its performance increases, causing its malfunction or damage, which is especially dangerous in critical systems, for example, in the space industry. Therefore, it is important to perform diagnostics of the developed REE to avoid possible faults and failures. This is especially important for printed circuit boards (PCB), because their conductors, in general, are placed arbitrarily. A special place in such diagnostics is taken by a computer simulation since it allows obtaining sufficiently correct information about REE with minimal effort and without carrying out a full-scale experiment.

One of the criteria for such diagnostics can be the amplitude criteria based on the *N*-norms that C. Baum proposed in 1979 [2]. To calculate them, you need to know the signal waveform in the time domain. To solve EMC problems, at the Tomsk State University of Control Systems and Radioelectronics (TUSUR) there has been developed [3]. In the TALGAT software, the possibility to calculate signal waveforms along the conductors of an arbitrary circuit consisting of multiconductor transmission line (MCTL) segments has been created on the basis of the theory from [4–6]. In addition, the possibility to calculate *N*-norms based on the obtained waveforms has been added recently. With the help of the implemented functionality, a number of investigations have been carried out: in the test circuits of single and coupled transmission lines, as well as the meander lines with one and two turns. Also, more complex circuits have been investigated [7]. One of them is a PCB bus of an autonomous navigation system (ANS) of a spacecraft. One of the important tasks was to diagnose the signal bus of the PCB for possible failures.

Nevertheless, the attention of the investigators is increasingly attracted to ultrashort pulse propagation along the spacecraft power supply bus. The software for calculating *N*-norms developed earlier can be used to carry out a comprehensive investigation of the power supply bus. For instance, it is interesting to investigate how the change in the pulse rise and fall times influences the operation of the spacecraft power supply bus. Therefore, the aim of this work is to investigate the influence of the change of ultrashort pulse rise and fall times on the *N*-norm portraits calculated along conductors of the spacecraft power supply bus.

II. Theory and Simulation Parameters

The theoretical basis and algorithms for calculating quasistatic response along each conductor of each multiconductor transmission line (MCTL) section connected to the multiconductor network were developed earlier [6, 8, 9] and are omitted here. A summary of the definitions of the N_1–N_5 norms is presented in Table I, reproduced from [2, 10]. The *N*-norms are parameters that are used to characterize a signal in the time domain and historically have been proposed to determine the limits of equipment susceptibility to external influences. A particular interest to the use of the norms is explained by the fact that they can be used to indicate the effect of the field on systems [2, 11]. The *N*-norms calculation is based on the application of mathematical operators to the entire signal waveform. It is necessary to calculate *N*-norm values in each segment along a conductor of each MCTL section in order to draw the *N*-norm portrait.

The structure to be studied was a spacecraft power supply bus. The solid model of the bus is shown in Fig. 1, and the circuit diagram—in Fig. 2. It is important to note that the bus

This research was funded by the Ministry of Science and Higher Education of the Russian Federation grant number 8.9562.2017/8.9 and the Russian Federation President grant MD-2652.2019.9.

in the circuit diagram is marked by a red color and consists of 4 MCTL sections.

TABLE I. *N*-NORM PARAMETERS: DESCRIPTION, AND APPLICATION

N-norm	Name	Application
$N_1 = \left\|R(t)\right\|_{\max}$	The peak (absolute) value	Circuit failure / electric breakdown / electric arc effects
$N_2 = \left\|\dfrac{\partial R(t)}{\partial t}\right\|_{\max}$	The peak (absolute) derivative	Component sparkling / circuit failure
$N_3 = \left\|\int_0^t R(t)dt\right\|_{\max}$	The peak (absolute) pulse	Dielectric breakdown (if *R* means the *E* field)
$N_4 = \int_0^t \left\|R(t)\right\| dt$	Rectified general pulse	Equipment damage
$N_5 = \left\{\int_0^\infty \left\|R(t)\right\|^2 dt\right\}^{\frac{1}{2}}$	The square root of the action integral	Component burn-out

Other MCTL sections are branch conductors of the power supply bus. The length of MCTL sections 1–4, and 13–16 is 0.5 m, 9–12 is 1 m, 5–8 is 0.03 m, 6 and 7 is 0.25 m. The cross-sections of the bus and branch conductors are shown in Figs. 3 and 4, respectively. The MCTL sections 5 and 8 have the cross-section from Fig. 3 *a*, 6 and 7 – Fig. 3 *b*, 1–4 and 13–16 from Fig. 4 *b*, and 9 and 12 – Fig. 4 *a*.

The dimensional specifications of the cross-sections are presented in Table II.

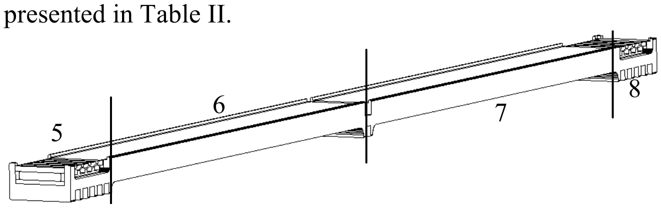

Fig. 1. Solid model of the power supply bus

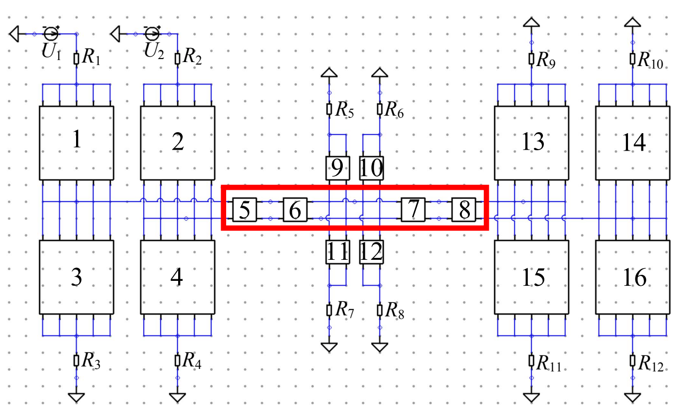

Fig. 2. Circuit diagram of the power supply bus and branch conductors

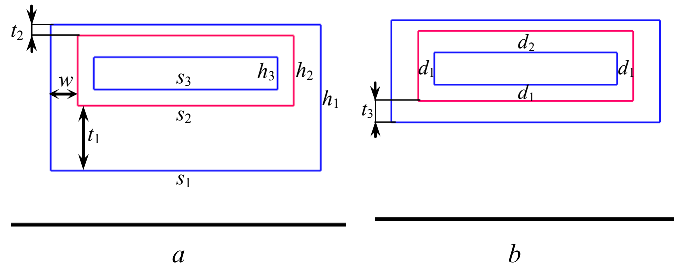

Fig. 3. Cross-sections of the power supply bus in its big (*a*), and small (*b*) parts

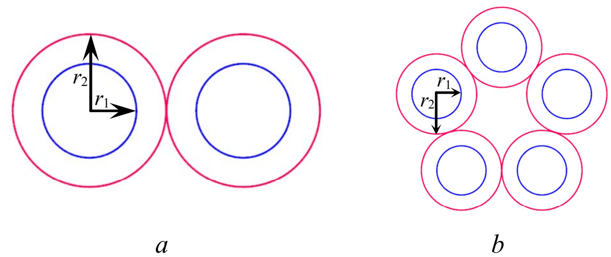

Fig. 4. Cross-sections of the central (*a*), and of the ends (*b*) brunch conductors

TABLE II. DIMENSIONAL SPECIFICATIONS OF THE CROSS-SECTIONS

Description	Notation	Value, mm
Width of the outside conductor	s_1	25
Dielectric width	s_2	20
Width of the inside conductor	s_3	17
Height of the outside conductor	h_1	13.5
Dielectric height	h_2	6.5
Height of the inside conductor	h_3	3
Lower thickness of the outside conductor in its big part (Fig. 3 *a*)	t_1	6
Higher thickness of the outside conductor	t_2	1
Lower thickness of the outside conductor in its small part (Fig. 3 *b*)	t_3	2
Thickness of the side wall of the outside conductor	w	2.5
Radius of the branch conductor	r_1	0.4
Radius of the dielectric across branch conductor	r_2	0.65

We used a common-mode excitation of the trapezoidal ultrashort pulse. Excitation sources (U_1 and U_2) are connected to MCTL sections 1 and 2 (as shown in Fig. 2). Electromotive force amplitude is 100 V. Flat top duration is 5 ns. The rise and fall times were changed (1 ns, 100 ps, and 10 ps). All resistors were 50 Ohm.

III. SIMULATION RESULTS

Each MCTL section is divided into 30 segments. A signal waveform was calculated in each segment between resistors R_1 and R_{11}. It was made in order to draw the *N*-norm portraits, i.e. to get an *N*-norm value variation along the conductor. Then, *N*-norm values were calculated and the portraits were drawn based on the calculated signal waveforms. After this, the excitation parameters were changed and the calculations repeated. The N_1 norm portraits are presented in Fig. 5, where *n* is a segment number along MCTL sections, $t_{r,f}$ is rise and fall duration times.

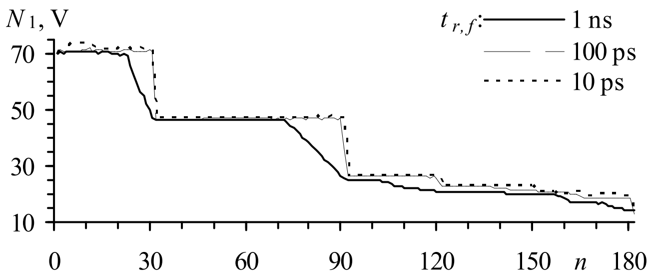

Fig. 5. N_1 norm portraits

The N_2-norm portraits are presented in Fig. 6. The enlarged fragment of this portrait is presented in Fig. 6 *b* (in order to see the case with 1 ns duration). The portraits of N_3–N_5 norms are presented in Fig. 7–9, respectively.

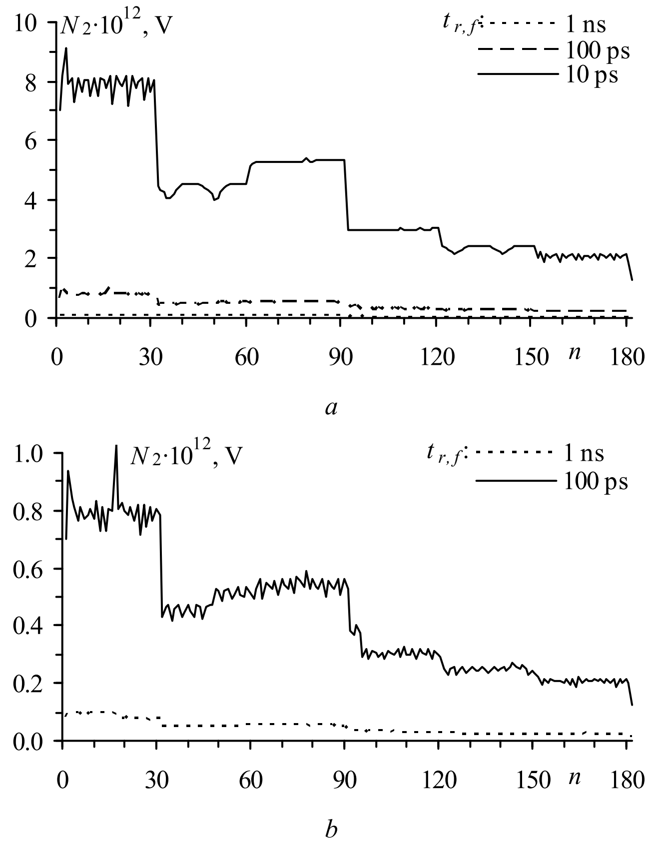

Fig. 6. N_2 norm portraits (*a*) and the enlarged fragment (*b*)

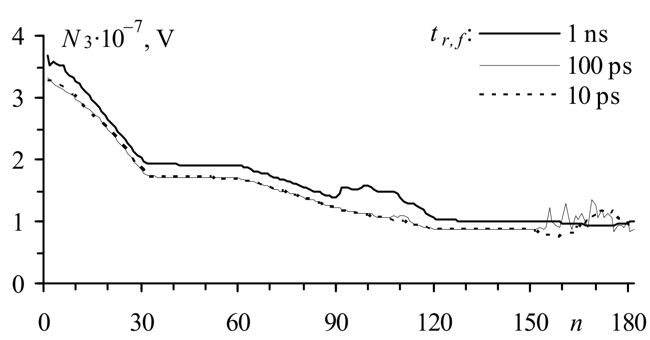

Fig. 7. N_3 norm portraits

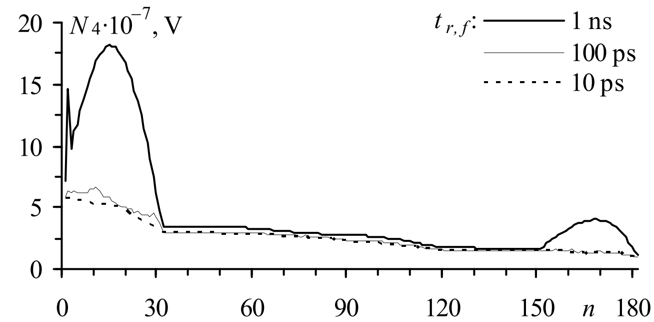

Fig. 8. N_4 norm portraits

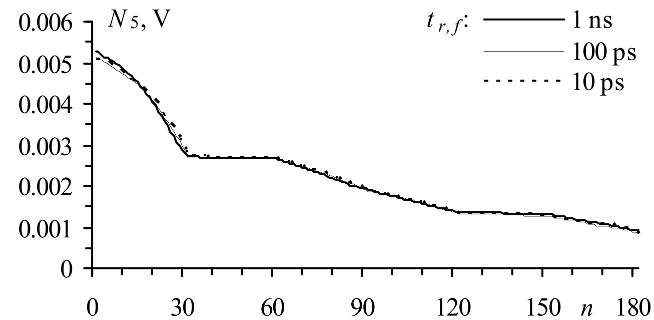

Fig. 9. N_5 norm portraits

IV. Discussion of Results

Consider the N_1 norm portraits. This norm shows the value of a voltage maximum. As can be seen from Fig. 5, the norm values at $t_{r,f}$=100 ps and 10 ps are almost similar, but for the case with $t_{r,f}$=1 ns they are different. Note a strong reduction of the norm value (for all $t_{r,f}$) in the vicinity of segments 30 and 90, which are the connection places of the branch conductors. But at segment 150, there is no such reduction.

Let us consider the N_2 norm portraits. The N_2 norm shows the possibility of the component sparking. This norm is much more exposed to the influence of rise and fall times, as we can see in Fig. 6 (the difference between values is up to 10 times). Thus, the shorter rise and fall times, the higher the possibility of component sparking. Like the N_1 norm, this norm has a reduction of the norm value near segments 30 and 90. The most vulnerable MCTL section is the first (segments 1–30).

Let us consider the N_3 norm portraits. This norm defines the dielectric breakdown. As can be seen from Fig. 7, the rise and fall times variation has hardly any influence on the norm value. The most dangerous place of the circuit is the beginning if the MCTL section (segments 1–5). The possibility of breakdown significantly reduces when propagating along the conductor.

Let us consider the N_4 norm portraits. The N_4 norm is used to detect equipment damage. As we can see in Fig. 8, the norm value is the highest when $t_{r,f}$=1 ns. The portrait has two strong peaks: the first is in the MCTL section 1 (segments 19, 20), and the second is in the last MCTL section (segments 169, 170). These MCTL sections are the branch conductors of the power supply bus. In other cases the norm values are close to each other and slightly decrease when propagating along the conductor.

Let us consider the N_5 norm portraits. The N_5 norm is used to detect a component burn-out. The variation of $t_{r,f}$ has hardly any influence on the norm value. The possibility of a burn-out is the highest in segment 1 and slightly decreases when propagating along the conductor.

V. Conclusion

Thus, we investigated the influence of rise and fall times on the *N*-norm portraits. It is shown that the highest influence of the rise and fall times is on the values of N_2 and N_4 norms (component sparking, equipment damage). This work also showed the possibility to reveal the most dangerous places along a chosen trace with defined excitations.

References

[1] S. Roy, A. Dounavis, “Macromodeling of multilayered power distribution networks based on multiconductor transmission line approach,” *IEEE Trans. on Components, Packaging and Manufacturing Technology*, vol. 3, pp. 1047–1056, 2013.

[2] Baum C 1979 Norms and Eigenvector Norms Mathematics Notes Note 63 1–42

[3] Kuksenko S P, Gazizov T R, Zabolotsky A M, Ahunov R R, Surovtsev R S, Salov V K, Lezhnin Eg V 2015 New developments for improved simulation of interconnects based on method of moments. Advances in Intelligent Systems Research Proc. of the 2015 Int. Conf. on Modelling, Simulation and Applied Mathematics (MSAM2015) 293–301.

[4] Djordjevic A R, Sarkar T K 1987 Analysis of time response of lossy multiconductor transmission line networks IEEE Trans. Microw. Theory Tech. 35(10) 898–907

[5] Zabolotsky A M 2016 Models, algorithms, methods, technologies and devices for electromagnetic compatibility providing of an onboard spacecraft radioelectronic equipment Doctoral dissertation Tomsk State University of Control Systems and Radioelectronics 295 p.

[6] Gazizov R R 2018 Mathematic model, numerical method, and software complex for revealing and localization of signal extremes in multiconductor transmission lines PhD dissertation Tomsk State University of Control Systems and Radioelectronics 224 p.

[7] R. R. Gazizov, B. S. Muhambetzhanova, T. T. Gazizov, and A.A. Kvasnikov, “Diagnostics of the printed circuit board bus of a spacecraft autonomous navigation system with using the *N*-norms,” *IOP Conf. Series: Materials Science and Engineering*, vol. 560, pp. 1–5, 2019

[8] A. M. Zabolotsky and T. R. Gazizov. *Time response of multiconductor transmission lines*. Tomsk: Tomsk State University, 2007, p. 152.

[9] R. Achar and M. S. Nakhla, “Simulation of high-speed interconnects,” *Proc. IEEE*, vol. 89, no. 5, pp. 693–728, 2001.

[10] Giri D 2004 High-power electromagnetic radiators : nonlethal weapons and other applications Cambridge, MA: Harvard University Press

[11] IEC "61000-4-33 2005 Electromagnetic compatibility (EMC) – Part 4-33: Testing and measurement techniques – Measurement methods for highpower transient parameters," ed: IEC